ADVANCED MATERIALS

130 nm, ~20 Ω □$^{-1}$) and SiO_2 (~15 nm) films. The deposition was performed by RF sputtering in 2.5 deposition cycles (1 cycle ≈ 0.8 μm) at a deposition rate of 1.5 nm s^{-1} and a pressure below 1.0×10^{-5} torr. Aluminum anodization was carried out in a 10 % phosphoric acid solution at 130 V and 7 °C. The TiO_2 sol (Sol. A, ~5 wt.-%) was prepared with titanium tetraisopropoxide, acetylacetone, distilled water, and ethanol at a mole ratio of 1:1:3:20, and the SiO_2–TeO_2 sol (Sol. B, ~5 wt.-%) with tetraethyl orthosilicate, telluric acid, ethanol, H_2O, and HCl at a mole ratio of 1:0.2:20:4:0.03. The composite TiO_2–SiO_2–TeO_2 sol was produced by adding 5–20 wt.-% of Sol. B to Sol. A. Other details of the sol synthesis are the same as in reference [21]. The morphology and the structural characteristics of the specimens were investigated by field emission scanning electron microscopy (FESEM) (S-5000, Hitachi), TEM (JEOL-100 kV), XRD (RINT-2200 V/PC, Cu Kα, 40 V/40 mA), and UV-vis spectrometry (U-3500, Hitachi). For TEM observation, the alumina/titania composite layers stripped from the substrates were embedded into epoxy resin and cut using an ultramicrotome (LKB-2088/V) with a diamond knife into ~60 nm thick slices. The sliced samples were set on carbon-coated copper micro-grids and observed in the bright field mode along with the corresponding diffraction patterns.

Received: May 21, 2002
Final version: September 9, 2002

[1] C. R. Martin, *Science* **1994**, *266*, 1961.
[2] S. Fan, M. G. Chapline, N. R. Franklin, T. W. Tombler, A. M. Cassell, H. Dai, *Science* **1999**, *283*, 512.
[3] M. Fu, Y. Zhu, R. Tan, G. Shi, *Adv. Mater.* **2001**, *13*, 1874.
[4] J. Bao, C. Tie, Z. Xu, Q. Zhou, D. Shen, Q. Ma, *Adv. Mater.* **2001**, *13*, 1631.
[5] B. C. Satishkumar, A. Govindaraj, E. M. Vogl, L. Basumallick, C. N. R. Rao, *J. Mater. Res.* **1997**, *12*, 604.
[6] C. Hippe, M. Wark, E. Lork, G. Schulz-Ekloff, *Microporous Mesoporous Mater.* **1999**, *31*, 235.
[7] M. Zhang, Y. Bando, K. Wada, *J. Mater. Res.* **2000**, *15*, 387.
[8] B. B. Lakshmi, P. K. Dorhout, C. R. Martin, *Chem. Mater.* **1997**, *9*, 857.
[9] B. B. Lakshmi, C. J. Patrissi, C. R. Martin, *Chem. Mater.* **1997**, *9*, 2544.
[10] T. Kasuga, M. Hiramatsu, M. Hirano, A. Honson, *J. Mater. Res.* **1997**, *12*, 607.
[11] D.-S. Seo, J.-K. Lee, H. Kim, *J. Cryst. Growth* **2001**, *229*, 428.
[12] J. H. Jung, H. Kobayashi, K. J. V. van Bommel, S. Shinkai, T. Shimizu, *Chem. Mater*. **2002**, *14*, 1445.
[13] S. M. Liu, L. M. Gan, L. H. Liu, W. D. Zhang, H. C. Zeng, *Chem. Mater*. **2002**, *14*, 1391.
[14] S. Z. Chu, K. Wada, S. Inoue, S. Todoroki, *J. Electrochem. Soc.* **2002**, *149*, B321.
[15] T. Kasuga, M. Hiramatsu, A. Honson, T. Sekino, K. Niihara, *Langmuir* **1998**, *14*, 3160.
[16] M. Zhang, Bando, K. Wada, K. Kurashima, *J. Mater. Sci. Lett.* **1999**, *18*, 1911.
[17] R. N. Viswanath, A. C. Bose, S. Ramasamy, *J. Phys. Chem. Solids* **2001**, *62*, 1991.
[18] H. Nakamura, Y. Matsui, *J. Am. Chem. Soc*. **1995**, *117*, 2651.
[19] S. Inoue, A. Nukui, in *The Physics of Non-Crystalline Solids* (Eds: L. D. Pye, W. C. La Course, H. J. Stevens), Taylor & Francis, London/Washington, DC **1992**, p. 281.
[20] S. Inoue, A. Nukui, in *Proc. Int. Conf. on Sci. & Tech. of New Glasses* (Eds: S. Sakka, N. Soga), Tokyo **1991**, p. 77.
[21] S. Z. Chu, K. Wada, S. Inoue, S. Todoroki, *Chem. Mater*. **2002**, *14*, 266.

A New Approach to Hybrid Polymer–Metal and Polymer–Semiconductor Particles

By *Jiguang Zhang*, *Neil Coombs*, *Eugenia Kumacheva*,* *Yuankun Lin*, and *Edward H. Sargent*

Recently, monodisperse polymer and silica microspheres have stimulated great interest in materials science. Their ability to organize in three-dimensional (3D) colloid crystals, whose periodicity is commensurate to the wavelength of light, is used in the fabrication of 3D photonic bandgap materials.[1] Following microbead assembly, the structure of colloid crystal is replicated in a high refractive index material,[2] after which the beads are removed. In another application, individual submicrometer particles are employed as templates for production of hollow microspheres with potential applications in drug delivery and as reactor or specific recognition systems. In this approach, inorganic, polymeric, or hybrid shells carrying useful functionalities are deposited onto the surface of a microsphere. In the next step, the particle core (generally of a polymeric nature) is dissolved. Shell attachment is accomplished using a layer-by-layer (LbL) strategy,[3] or by depositing small nanoclusters of the shell-forming material followed by their coalescence.[4] Finally, submicrometer particles can be used in their own right—as building blocks of periodic nanostructured materials. Such materials can have properties of photonic crystals and can be used in optical data storage, chemical sensors, and optical limiters and switches.[5] Furthermore, microbeads can have a core–shell morphology or a multilayer structure, which would lead to complex compositional and structural patterns in the ultimate nanocomposite material.[6]

In the last approach, the incorporation of semiconductor or metal nanoparticles (NPs) in submicrometer spheres is particularly attractive. The optical properties of the NPs (e.g., optical nonlinearity or photoluminescence) can be enhanced through resonance with the structural periodicity of the material on the scale of the optical wavelength. Preformed NPs have been incorporated in submicrometer beads during their synthesis,[7] or have been attached to the microbead surface through controlled heterocoagulation[8] and by means of LbL deposition.[3,9] In all these methods the main challenges were to control the size of NPs and their uptake by microspheres, along with control of colloid stability and monodispersity of the modified silica or polymer particles. These features determined the possibility of the further use of the modified microspheres as the building blocks of periodically structured materials.

[*] Dr. E. Kumacheva, J. Zhang, Dr. N. Coombs
Department of Chemistry, University of Toronto
80 Saint George Street, Toronto, ON M5S 3H6 (Canada)
E-mail: ekumache@chem.utoronto.ca
Dr. Y. Lin, Dr. E. H. Sargent
Edward S. Rogers Sr. Department of Electrical and Computer Engineering, University of Toronto
10 King's College Rd, Toronto, ON M5S 3G4 (Canada)

  0935-9648/02/2312-1756 $ 17.50+.50/0

Herein, we describe a strategy for production of monodisperse polymer microspheres coated with semiconductor (CdS) or metal (Ag) nanocrystals. In the first step, we employed an ion exchange between the counter ions in the electric double layer of the latex microbeads and Cd^{2+} or Ag^{+} ions. In the second step, CdS or Ag nanoparticles were formed by treating the latex dispersion with Na_2S or $NaBH_4$, respectively. A similar method was recently demonstrated for the preparation of Ag and PbS NPs in polyelectrolyte multilayers adsorbed on flat surfaces by a LbL technique,[10] However, in the present work, ion exchange of NPs was conducted directly in the electrical double layer of the microspheres, which were later used in the fabrication of photonic crystals.

Poly(methyl methacrylate)–poly(methacrylic acid) (PMMA–PMAA) latex particles, with polydispersity 1.05, average diameter varying from 150 to 600 nm, and the weight ratio of PMMA/PMAA varying from 10:1 to 4:1 were synthesized via emulsion polymerization.[6] For each dispersion, the concentration of surface COO^{-} groups was determined by titration of the latex by 0.1 M KOH solution. For example, for 600 nm particles and a PMMA/PMAA weight ratio of 5:1, the concentration of the surface COO^{-} groups was 5 mol.-% of their total concentration.

The PMMA/PMAA dispersion with particle concentration about 20 wt.-% was treated with 0.1 M KOH solution, and then dialyzed to pH 8.5. In the next step, the dispersion was treated with a 1 M solution of $Cd(ClO_4)_2$ in different molar ratios of Cd^{2+} to surface COO^{-} groups to provide ion-exchange between K^{+} counter ions in the double electric layer of the latex particles, and Cd^{2+} ions bearing a higher charge.[11] After 4 h stirring, the dispersion was repeatedly centrifuged to settle modified particles, and redispersed in the deionized water to remove excess Cd^{2+} ions. A 1 M solution of Na_2S was then slowly introduced into the dispersion. The color of the latex instantly became yellow, indicating the formation of CdS. The dispersion was again purified by centrifugation to remove CdS nanoparticles weakly attached to the polymer surface. After 2–3 cycles of centrifugation the supernatant became colorless, while the latex particles remained yellow, indicating that CdS NPs were strongly bound to the latex surface. The dispersion of the composite CdS–latex particles remained stable and particle polydispersity did not exceed 1.1.

The approach to coating of the microbeads with Ag NPs was similar to that used for CdS–PMMA/PMAA microbeads. Following addition of KOH and dialysis, the latex dispersion was treated with a 0.1 M solution of $AgNO_3$. After several centrifugation–redispersion cycles, Ag^{+} ions on the latex surface were reduced at 0 °C using a freshly prepared 1 mM solution of $NaBH_4$. The dispersion instantly changed color from white to dark-brown. After removing the unattached Ag nanoparticles, the hybrid microbeads had polydispersity of 1.2.

Figures 1a and 1e show transmission electron microscopy (TEM) images of hybrid 320 nm microspheres, uniformly coated with CdS and Ag NPs, respectively. Image analysis of the TEM micrographs showed that the surface coverage of the latex surface with the NPs could reach ca. 40 %. A fragment of the latex surface coated with CdS NPs is shown in Figure 1b. The size of the CdS NPs varied from ca. 4 to 7 nm. Figure 1f shows a fragment of the surface of a latex microsphere coated with 4–5 nm sized Ag NPs. For both CdS and Ag NPs, the size of nanocrystals and their concentration on the microsphere surface could be controlled by varying concentration of PMAA in the latex beads, and by changing the ratio of Cd^{2+} or Ag^{+} to surface COO^{-} groups.

The composition of the NPs synthesized on the latex surface was examined using energy dispersive X-ray (EDX) analysis. Figure 1c shows the results of surface mapping of the fragment shown in Figure 1b. A good correlation was obtained between the TEM image and the EDX map showing the localization of cadmium on the surface. The results of surface mapping with respect to sulfur were less conclusive. A strong "background" sulfur signal was obtained, due to the presence of SO_4^{2-} groups on polymer chains anchored to the particle surface, since $K_2S_2O_4$ was used as the initiator in latex polymerization. Figure 1g shows the results of surface mapping of the surface fragment shown in Figure 1f. The correlation between the Ag map and the TEM image was very good. Figures 1d and 1h show high resolution TEM images of the individual crystalline CdS and Ag NPs, respectively. The periodic dot pattern arises from the coherent imaging of Cd and S atoms (Fig. 1d) or Ag atoms (Fig 1h) making up the nanoparticle.

The size of Ag and CdS NPs was further characterized by UV-vis spectroscopy. To suppress strong light scattering, aque-

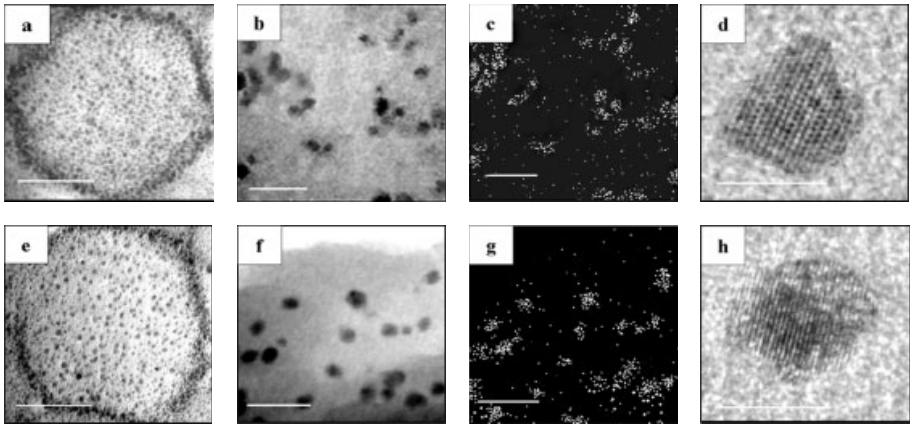

Fig. 1. TEM micrographs of PMMA–PMAA beads covered with CdS (a–d) and Ag (e–h) NPs. Weight ratio is 5:1 PMMA/PMAA and the concentration of the surface COO^{-} groups is 4.8 mol.-%. a,e) Individual latex microspheres coated with CdS (a) and Ag (e) NPs. Scale bar is 100 nm; b,f) Fragment of the latex surface covered with CdS (b) and Ag (f) NPs. Scale bar is 20 nm; c,g) Surface map of the coated microbead surface with respect to Cd (c) and Ag (g). Scale bar is 20 nm; d,f) High resolution image of individual CdS (d) and Ag (f) NPs. Scale bar is 5 nm.

  0935-9648/02/2312-1757 $ 17.50+.50/0

ADVANCED MATERIALS

ous dispersions of hybrid particles were strongly diluted by dimethyl sulfoxide (refractive index = 1.4790). The absorption spectrum of the CdS NPs synthesized on the surface of PMMA–PMAA beads is shown in Figure 2a. The maximum of 480 nm on the absorption peak corresponds to the average size of CdS NPs of ca. 5.0 nm, while the position of the absorption edge of

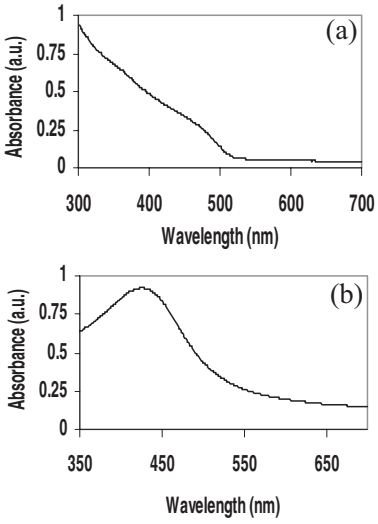

Fig. 2. UV-vis spectra of CdS (a) and Ag (b) nanoparticles formed on the surface on latex beads for PMMA/PMAA weight ratio 5:1. To minimize strong light scattering, hybrid beads were dispersed in DMSO.

ca. 515 nm gives the largest size of CdS NPs at ca. 6.8 nm,[12,13] in reasonable agreement with the results obtained by TEM. Figure 2b shows the UV-vis spectrum of Ag nanoparticles. The position of the peak of 430 nm for surface plasmon absorbance was close to the value measured by Asher et al.[14] and Bruening et al.[10] for 2–5 nm sized Ag quantum dots.

The advantage of in-situ synthesis of CdS and Ag NPs was that the hybrid microbeads retained the ability to form large-area mono- and multilayer ordered colloid arrays.[15–17] This feature distinguished the resulting microbeads from LbL-modified particles, in which a relatively soft shell formed by polyelectrolyte layers and substantial surface roughness of the microbeads[18] could impede particle assembly in large colloid crystals. Figure 3a shows the scanning electron microscopy (SEM) image of the colloid crystal formed by hybrid CdS–PMMA/PMAA particles, following their sedimentation under gravity. While this method is not ideal for the preparation of colloid crystals, good particle ordering obtained over areas exceeding 40 μm × 60 μm was achieved after deliberate removal of electrolytes from the dispersion. This feature suggested that electrostatically driven repulsion between hybrid microbeads strongly influenced the process of self-assembly. Indeed, after synthesis of the NPs, the electrokinetic potential, ξ, of the modified latex particles varied from –20 to –45 mV at pH 7.4. Although these values were lower than $\xi = -60$ mV measured for the corresponding bare latex particles, the electrostatic repulsion arising from free surface COO^- groups (as well as from the surface SO_4^{2-} groups) was sufficient to suppress particle aggregation prior to their assembly on the sub-

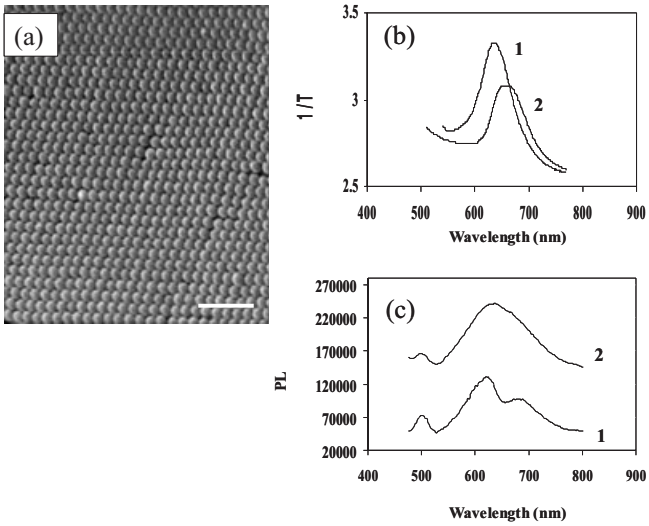

Fig. 3. a) SEM image of the multilayer array of CdS-doped PMMA/PMAA latex beads. Scale bar is 2.5 μm. b) Reciprocal of optical transmission of the colloid crystal fabricated from bare (curve 1) and CdS-coated (curve 2) microspheres. c) Photoluminescence of CdS nanoparticles in the colloid crystal prior to (curve 1) and after (curve 2) infiltration with DMSO. PL was excited with He-Cd laser at $\lambda = 442$ nm. PMMA/PMAA weight ratio is 5:1.

strate. In addition, Ag NPs could contribute to the negative charge of the latex microspheres.[7]

Since colloid arrays formed from hybrid CdS–PMMA/PMAA microspheres have potential applications as photonic crystals, their optical properties were studied by measuring their transmission and luminescence. Figure 3b shows optical transmission spectra measured at normal incidence ($\theta = 0°$) to the (111) plane of the colloid crystals fabricated from the uncoated (curve 1) and CdS-coated (curve 2) microspheres. For the array of 285 nm PMMA/PMAA microspheres, a diffraction peak appeared at 631 nm, whereas when the same spheres were doped with CdS NPs, the peak shifted to 656 nm. For such crystals the relation between the spectral position of the diffraction peak, λ_c, and the effective refractive index, n_{eff}, is defined by $\lambda_c = 1.632\, n_{eff}\, D$[19], where D is the diameter of a microsphere. Since the colloid crystals obtained from the modified and uncoated microbeads had a similar lattice constant, we estimated a 4 % increase in effective refractive index, in comparison with the array formed by unmodified PMMA/PMAA beads. The effective refractive indices of the bare and CdS-coated particles were 1.357 and 1.410, respectively. The fraction of CdS NPs in the latex microspheres was estimated from this measured value of n_{eff} of the CdS-doped colloid crystal. We assumed the volume fraction of PMMA–PMAA beads to be 74 %, and used the relationship $n_{eff}^2 = 0.26 n_a^2 + n_{PMMA/PMAA}^2 (0.74 - f) + n_{NP}^2 f$[19] where n_a, $n_{PMMA/PMAA}$, and n_{NP} are the refractive indices of air, PMMA/PMAA, and CdS, respectively, and f is the volume fraction of CdS in the colloid crystal. For $n_{PMMA/PMAA} = 1.491$ and $n_{NP} = 2.5$, f was found to be 0.021 and the CdS/polymer volume ratio in the microspheres was 2.9 vol.-%.

Figure 3c shows photoluminescence (PL) spectra of CdS NPs coating PMMA–PMAA microspheres, before and after

  0935-9648/02/2312-1758 $ 17.50+.50/0 *Adv. Mater.* **2002**, *14*, No. 23, December 3

infiltration of the colloid crystalline array with dimethyl sulfoxide (DMSO). The PL spectrum of CdS NPs features band-edge emission at 480 nm, close to the onset of absorption, and a broad peak in the range 560–740 nm, attributed to the recombination of charge carriers in deep traps of surface localized states.[18] Prior to infiltration of the colloid crystal with DMSO, a spectral dip in the spectrum occurred at 650 nm for PL collected perpendicular to the (111) plane of the colloidal crystal (bottom curve). The spectral position of the dip corresponded to the centre of the diffraction peak obtained for CdS-doped colloid crystal (Fig. 2b, bottom curve). When the crystal was infiltrated with index-matching DMSO, the dip in the PL spectrum disappeared as a result of the loss of strong diffraction within the colloid crystal. These results gave evidence of coupling between the structurally and compositionally driven optical properties of the colloid array produced from hybrid microspheres.

The strategy described in this work opens in a new avenue for production of polymer submicrometer size particles coated with semiconductor and metal NPs. A sufficiently smooth surface, a significant surface charge, and a strong attachment of the NPs to the latex surface, provides growth of high quality colloid crystalline arrays, a vital condition for production of photonic crystals. Good control over the diameter of NPs determines their confined electronic states, and consequently the spectral properties of their interactions with light, via the quantum size effect.[20]

While high-density doping of the colloid crystal with NPs can be used as a strategy to achieve high refractive index contrast towards a full photonic bandgap,[21] the present work reports progress at the other end of the doping density spectrum. Lasers based on photonic crystals require controlled gain per unit length: today's semiconductor lasers typically target a ~1–5 % overlap factor between optical mode and gain-producing active materials.[22] Devices for processing optical signals in the time domain require control over both linear and nonlinear refractive index (Kerr coefficient) which demands a few percent doping with nanocrystals.[23]

The experimental proof of interaction between nanoscale engineering of electronic bandstructure, and submicrometer-scale engineering of photonic bandstructure, lies in our observation of photoluminescence influenced by photonic crystal Bragg diffraction.

Experimental

Surface concentration of carboxyl groups in the latex beads was determined by titrating 10 mL of PMMA/PMAA dispersion (solid content 5–20 wt.-%) with 0.1 M KOH. Potentiometric signals were recorded 5 min after each dosage, using an inline MV III-SC pH meter (Malvern Instruments, UK) portable pH meter. The same instrument was used to determine particle size and electrokinetic potential.

A Hitachi S-570 scanning electron microscope was used to characterize the morphology and organization of the modified PMMA/PMAA particles. The accelerating voltage was 15 kV, and the working distance used was 1 mm. TEM measurements were carried out on a Hitachi model 600 electron microscope with 70 kV accelerating voltage. A small drop of the dispersion was placed on a Cu grid covered with carbon film and after 1 min the excess of the liquid was removed. The sample was in air before introduction into the electron microscope. High resolution TEM images were obtained using a JEOL 2010F microscope operating at 200 kV. UV-vis spectra were taken on Cary 500 spectrophotometer. Photoluminescence measurements were taken with a PTI spectrofluorometer.

Received: May 28, 2002
Final version: August 27, 2002

[1] S. John, *Phys. Rev. Lett*. **1987**, *58*, 2486.
[2] a) B. T. Holland, C. F. Blanford, A. Stein, *Science* **1998**, *281*, 538. b) A. A. Zahidov, R. H. Baughman, Z. Iqbal, C. Cui, I. Khayrullin, S. O. Dantas, J. Marti, V. G. Ralchenko, *Science* **1998**, *282*, 897. c) J. E. G. Wijnhoven, W. L. Vos, *Science* **1998**, *281*, 802.
[3] a) G. Decher, *Science* **1997**, *277*, 1232. b) F. Caruso, R. A. Caruso, H. Möhwald, *Science* **1998**, *282*, 1111. c) F. Caruso, *Adv. Mater*. **2001**, *13*, 11.
[4] C. Graf, A. van Blaaderen, *Langmuir* **2002**, *18*, 524.
[5] a) B. J. Siwick, O. Kalinina, E. Kumacheva, R. J. D. Miller, J. Noolandi, *J. Appl. Phys.* **2001**, *90*, 5328. b) K. Lee, S. A. Asher, *J. Am. Chem. Soc.* **2000**, *122*, 9534. c) L. Brzozowski, E. H. Sargent. *IEEE J. Quantum Electron*. **2000**, *36*, 550.
[6] a) O. Kalinina, E. Kumacheva, *Macromolecules* **1999**, *32*, 4122. b) O. Kalinina, E. Kumacheva, *Macromolecules* **2002**, *35*, 3675. c) O. Kalinina, E. Kumacheva, *Chem. Mater.* **2001**, *13*, 35.
[7] a) S.-Y. Chang, L. Liu, S. A. Asher, *J. Am. Chem. Soc.* **1994**, *116*, 6739. b) X. L. Xu, G. Friedman, K. D. Humfeld, S. A. Majetich, S. A. Asher, *Chem. Mater*. **2002**, *14*, 1249.
[8] a) J. Han, E. Kumacheva, *Langmuir* **2001**, *17*, 7912. b) K. Furusawa, O. D. Velev, *Colloids Surf.* **1999**, *159*, 359.
[9] a) F. Caruso, H. Möhwald, *Langmuir* **1999**, *15*, 8276. b) A. Rogach, A. Susha, F. Caruso, G. Sukhorukov, A. Kornowski, S. Kershaw, H. Möhwald, A. Eychmüller, H. Weller, *Adv. Mater*. **2000**, *12*, 333.
[10] a) S. Joly, R. Kane, L. Radzilowski, T. Wang, A. Wu, R. E. Cohen, E. L. Thomas, M. F. Rubner, *Langmuir* **2000**, *16*, 1354. b) J. Dai, M. L. Bruening, *Nano Lett.*, in press.
[11] P. C. Hiemenz, *Principles of Colloid and Surface Chemistry*, 2nd ed., Marcel Dekker, NewYork **1986**, p. 815.
[12] L. Spanhel, M. Haase, H. Weller, A. Henglein, *J. Am. Chem. Soc.* **1987**, *109*, 5649.
[13] M. Moffitt, H. Vali, A. Eisenberg, *Chem. Mater*. **1998**, *10*, 1021.
[14] W. Wang, S. A. Asher, *J. Am. Chem. Soc.* **2001**, *123*, 12 528.
[15] Another advantage of this method is the possibility to attach the second polymeric shell using emulsion polymerization, and thus produce a nanocomposite material as described in [6].
[16] Further control of colloid crystal growth could be achieved by electrodeposition on mesoscopically patterned surfaces [17].
[17] E. Kumacheva, R. Golding, M. Allard, E. H. Sargent, *Adv. Mater*. **2002**, *14*, 221.
[18] R. A. McAloney, M. Sinyor, V. Dudnik, C. M. Goh. *Langmuir* **2001**, *17*, 6655.
[19] A. Blanco, C. López, R. Mayoral, H. Míguez, F. Meseguer, A. Mifsud, J. Herrero, *Appl. Phys. Lett*. **1998**, *73*, 1781.
[20] Y. Lin, J. Zhang, E. H. Sargent, E. Kumacheva, *Appl. Phys. Lett.*, in press.
[21] Y. A. Vlasov, N. Yao, D. J. Norris, *Adv. Mater*. **1999**, *11*, 165.
[22] E. H. Sargent, *Solid-State Electron.* **2000**, *44*, 147.
[23] L. Brzozowski, E. H. Sargent, *IEEE J. Quantum Electron*. **2000**, *36*, 550.

  0935-9648/02/2312-1759 $ 17.50+.50/0